

Input-output Feedback Linearization Control for SM-PMSM

Senhaji Abdelhamid^{1,*}, *Abdelouhab Mostafa*¹, *Attar Abdelilah*¹, *Amri Lahcen*¹ and *Bouchnaif Jamal*¹

¹Laboratory of Electrical Engineering and Maintenance, Higher School of Technology, Mohammed First University, Oujda, Morocco

Abstract. This paper introduces a velocity control strategy for Surface-Mounted Permanent Magnet Synchronous Motors SM-PMSM using exact linearization and input-output decoupling techniques, which are rooted in the principles of differential geometry. The primary aim of this control approach is to establish a static state feedback mechanism and to convert the nonlinear PMSM model into a linear, decoupled, and controllable system. Initially, the state model that represents the PMSM dynamics within the $d-q$ reference frame is defined. Subsequently, the process of designing the control through linearization and input-output decoupling is outlined. Lastly, the synthesis of the compensator is grounded in the pole placement method, aiming to drive the direct current towards zero and ensure optimal torque operation. Simulation outcomes conducted on Matlab/Simulink demonstrate the efficacy of the speed control strategy, which is facilitated by a straightforward algorithm for practical implementation. However, it is inadequate against variations in machine parameters and load torque disturbances.

Keywords. speed control, SM PMSM, linearization, input-output decoupling, differential geometry, pole placement method.

1 Introduction

The Permanent Magnet Synchronous Motor (PMSM) has made significant progress in the field of electrical engineering, through various applications industries and systems where precise control and high efficiency are required. Here are some areas of use and a possible application for PMSM with linearization feedback control: in robotic arms for precise positioning, in aerospace and aviation such as actuating flaps, ailerons, and rudders, in electric vehicles for propulsion, in renewable energy, PMSM are used in wind turbines for converting wind energy into electricity, also in medical devices where Precision and stability are crucial in medical imaging equipment like magnetic resonance imaging machines [1–3]. This type of motor offers exceptional superior performances due to its energy efficiency,

* Corresponding author: a.senhaji@ump.ac.ma

excellent dynamic performance, allowing it to maintain an almost constant torque over a wide range of speeds, as well as great durability thanks to its improved efficiency resulting from reduced internal losses [4,5]. They are therefore better suited to applications requiring variable speed, unlike induction or DC motors. However, despite the design of powerful processing boards, several challenges persist in the control of PMSM [6]. Namely, the mathematical model is highly non-linear and the complex dynamics of PMSM require sophisticated control algorithms to achieve optimum performance, sensitivity to load torque variations and disturbances, and synchronizing stator current and rotor position requires constant attention, particularly at high speeds [4,6–8].

In the paper [9], differential geometry was used to achieve accurate feedback loop linearization for the PMSM, and decoupling between the speed loop and the current loop, with active disturbance rejection, was achieved. Furthermore, the controller has been developed to adjust gains finely as a function of error. Simulation results show that speed tracking is fast and stable, without any effect on the direct axis current. The same study, based on the differential geometry approach, has been presented in several research publications[4,10]. The focus has always been on controlling the PMSM using exact input-output linearization via state feedback. As this method relies on the full elimination of non-linearities in the model, it results in a wide speed control range, fast response and low steady-state error. However, the weaknesses of this method are its strong dependence on system parameters, making it sensitive to parameter variations[11,12].

In contrast, the backstepping method provides a choice for synthesizing a controller which considers both parametric uncertainties and unknown disturbances [3,13,14]. Several recent researches have seen the light of day in the design of advanced controllers, such as adaptive backstepping control [8,15,16], sliding mode control SMC [17,18], direct torque control DTC [19,20] and active disturbance rejection control ADRC [21,22]. In the wake of the development of artificial intelligence and fuzzy logic algorithms, sophisticated and robust controllers for PMSM have been designed [23,24].

The purpose of this paper is to develop an algorithm to control the speed and current of the PMSM using the technique of exact linearization and input-output decoupling. As in[11,25,26], this means transforming the non-linear PMSM model into a decoupled, controllable and linear model using static state feedback. In this new coordinate system, the convergence of speed to the desired value ω_{ref} and direct current to the desired value $i_{d.ref} = 0$, is guaranteed by pole placement. The following work is structured as follows. Section 2 shows the dynamic model of the PMSM in the d-q frame. The input-output linearization method and the stabilization of the controller by pole placement are developed in Section 3. The fourth section presents the block diagram of the whole system and the simulation results obtained using MATLAB/Simulink software. Finally, conclusion and prospects are provided in Section 5.

2 PMSM dynamic model

The representation of the state model for the surface-mounted permanent magnet synchronous motor SM-PMSM in the d-q frame is outlined as follows:

$$\frac{d\omega_r}{dt} = \frac{3p^2\phi_r}{2J} i_q - \frac{B}{J} \omega_r - \frac{pT_L}{J} \quad (1)$$

$$\frac{di_d}{dt} = -\frac{R_s}{L_s} i_d + \omega_r i_q + \frac{u_d}{L_s} \quad (2)$$

$$\frac{di_q}{dt} = -\frac{R_s}{L_s} i_q - \omega_r i_d - \frac{\phi_r}{L_s} \omega_r + \frac{u_q}{L_s} \quad (3)$$

Here, R_s represents the stator resistance, L_s stands for the d-q axis inductances, i_d, i_q, u_d and u_q correspond to the stator currents and voltages in the d-q axis. Additionally,

p denotes pole pairs number, while ω_r and φ_r refer to the rotor's electrical angular speed and flux, T_L represents the load torque, which will be treated as a disturbance. Furthermore, J represents the rotor inertia, and B signifies the viscous friction coefficient [14]. In order to design control laws based on input-output linearization feedback, the following assumptions are retained:

- **A1:** All motor parameters are assumed to remain constant and known.
- **A2:** All state variables ω_r, i_d and i_q are available for feedback.
- **A3:** The signal $\omega_{r,d} \in \mathfrak{R}$ represents the trajectory of the desired reference speed, which can be differentiated numerically and bound by the following derivatives $\omega_{r,d}, \dot{\omega}_{r,d}, \ddot{\omega}_{r,d} \in L_\infty$.

The third-order model of PMSM is strongly nonlinear and can be represented in affine form by the command as follows:
$$\begin{cases} \dot{x} = f(x) + g(x)u \\ y = h(x) \end{cases}$$

Where: $x = [\omega_r \quad i_d \quad i_q]^T = [x_1 \quad x_2 \quad x_3]^T$ is the state vector, $u = \begin{pmatrix} u_q \\ u_d \end{pmatrix} = \begin{pmatrix} u_1 \\ u_2 \end{pmatrix}$ is the control input, y is the output to be controlled, the functions $f(x)$, $g(x)$ and $h(x)$ are analytic:

$$f(x) = \begin{bmatrix} f_1(x) \\ f_2(x) \\ f_3(x) \end{bmatrix} = \begin{bmatrix} a_1 x_3 - a_2 x_1 - a_3 T_L \\ -b_1 x_2 + x_1 x_3 \\ -c_1 x_3 - x_1 x_2 - c_2 x_1 \end{bmatrix}, \quad g(x) = [g_1(x) \quad g_2(x)] = \begin{bmatrix} 0 & 0 \\ 0 & \frac{1}{L_s} \\ \frac{1}{L_s} & 0 \end{bmatrix}$$

$$y = \begin{pmatrix} h_1(x) \\ h_2(x) \end{pmatrix} = \begin{pmatrix} y_1 \\ y_2 \end{pmatrix} = \begin{pmatrix} x_1 \\ x_2 \end{pmatrix} = \begin{pmatrix} \omega_r \\ i_d \end{pmatrix}$$

With: $a_1 = \frac{3p^2 \varphi_r}{2J}; a_2 = \frac{B}{J}; a_3 = \frac{p}{J}; b_1 = \frac{R_s}{L_s}; c_1 = b_1; c_2 = \frac{\varphi_r}{L_s}$ (4)

The electromagnetic torque is given by the following relationship: $T_e = \frac{3}{2} p \varphi_r i_q$ (5)

3 Controller design

3.1 Linearization exact and Input-Output decoupling

The objective is to try to synthesize a static state feedback to compensate the non-linearities of the PMSM model, such as: $u = \alpha(x) + \beta(x)v$, with $v = \begin{pmatrix} v_1 \\ v_2 \end{pmatrix}$ is the new external control input that stabilizes the system. This will establish a linear relationship between v and the output y . Afterwards a change of coordinates $z = \Phi(x)$ is necessary to transform the PMSM model into a linear and controllable system in condensed canonical form:
$$\begin{cases} \dot{z} = Az + Bv \\ y = Cz \end{cases}$$

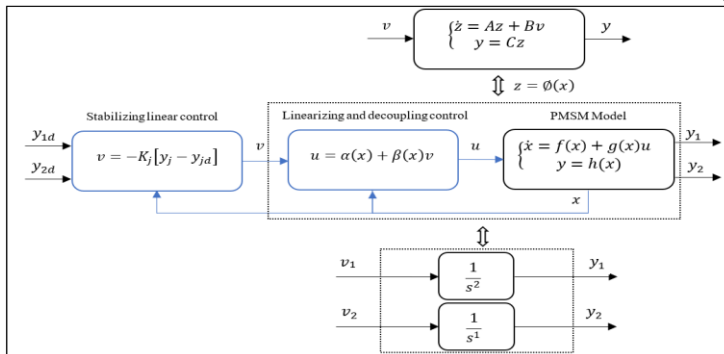


Fig 1. Architecture of the control by linearization and input-output decoupling

All these steps are illustrated in the Figure 1.

The principle is simple, we derive the output until a component of the control vector appears:

- For the speed, from (1) and (4): $y_1 = x_1 = \omega_r \Rightarrow \dot{y}_1 = a_1x_3 - a_2x_1 - a_3T_L$

The second derivative is obtained by replacing (3) and (4) in the last equation:

$$\ddot{y}_1 = a_1(-c_1x_3 - x_1x_2 - c_2x_1) - a_2(a_1x_3 - a_2x_1 - a_3T_L) + a_1\frac{u_1}{L_s} \quad (6)$$

The relative degree [number of times the output must be derived to explicitly show at least one component of the control vector] of the output y_1 is: $r_1 = 2$

- For the direct current, from (2) and (4):

$$y_2 = x_2 = i_d \Rightarrow \dot{y}_2 = -b_1x_2 + x_1x_3 + \frac{u_2}{L_s} \quad (7)$$

Hence the relative degree for the output y_2 is therefore: $r_2 = 1$

Then, the decoupled system is presented as a set of two single-input single-output SISO subsystems; in this way, the control input v_1 only affects the speed of the PMSM and v_2 controls the direct current i_d , as shown in Fig 1.

For both outputs y_1 and y_2 , (6) and (7) can be written as a matrix:

$$\begin{pmatrix} \ddot{y}_1 \\ \dot{y}_2 \end{pmatrix} = \Delta_0(x) + \Delta(x) \times \begin{pmatrix} u_1 \\ u_2 \end{pmatrix} = \begin{pmatrix} v_1 \\ v_2 \end{pmatrix} \quad (8)$$

$$\Delta_0(x) = \begin{bmatrix} a_1(-c_1x_3 - x_1x_2 - c_2x_1) - a_2(a_1x_3 - a_2x_1 - a_3T_L) \\ -b_1x_2 + x_1x_3 \end{bmatrix} \text{ and } \Delta(x) = \begin{pmatrix} \frac{a_1}{L_s} & 0 \\ 0 & \frac{1}{L_s} \end{pmatrix}$$

The determinant of the uncoupling matrix $\Delta(x)$ is calculated:

$$\det(\Delta(x)) = \frac{a_1}{L_s^2} \neq 0 \Rightarrow a_1 \neq 0 \Rightarrow \varphi_r \neq 0$$

$\Delta(x)$ is not singular, then the dynamic state model of the permanent-magnet synchronous motor is decoupled by static state feedback:

$$u = \alpha(x) + \beta(x)v = \Delta^{-1}(x) \times (-\Delta_0(x) + v)$$

Where:

$$\alpha(x) = -\Delta^{-1}(x) \times \Delta_0(x) \text{ and } \beta(x) = \Delta^{-1}(x)$$

The dimension of the PMSM after looping is: $r = r_1 + r_2 = n = 3$, so the system is completely linearizable. The input-output behavior of the looped system is linear and described by a chain of integrators (see Fig 1): $\frac{Y_1(s)}{V_1(s)} = \frac{1}{s^2}$ and $\frac{Y_2(s)}{V_2(s)} = \frac{1}{s}$

3.2 Poles placement control

The second loop involves building the control v which stabilizes the speed and current of the PMSM and enables the reference settings to be followed:

$$y_{1d} = \omega_{r,d} \text{ and } y_{2d} = i_{d,d} = 0$$

We define the tracking error for the speed ω_r as follows:

$$\varepsilon_1 = y_1 - y_{1d} = \omega_r - \omega_{r,d} ; \dot{\varepsilon}_1 = \varepsilon_{12}$$

we obtain: $\begin{cases} \dot{\varepsilon}_1 = \varepsilon_{12} \\ \dot{\varepsilon}_{12} = v_1 - \ddot{y}_{1d} = \bar{v}_1 \end{cases} \Rightarrow \{\dot{\varepsilon}_1 = A_1\varepsilon_1 + B_1\bar{v}_1$

The command v_1 is chosen such that:

$$\bar{v}_1 = -k_1\varepsilon_1 \Rightarrow v_1 = -k_1\begin{pmatrix} y_1 - y_{1d} \\ \dot{y}_1 - \dot{y}_{1d} \end{pmatrix} + \ddot{y}_{1d} \quad (9)$$

Similarly, the tracking error for the direct current i_d is given by:

$$\varepsilon_2 = y_2 - y_{2d} = i_d - i_{d,d}$$

The command v_2 is chosen such that:

$$v_2 = -k_2(y_2 - y_{2d}) + \dot{y}_{2d} \quad (10)$$

The vector k_j is chosen such that the real part of the eigenvalues of the matrix $(A_j - B_j k_j)$ is strictly negative: $Re[eigv(A_j - B_j k_j)] < 0 ; j = 1,2$

$$A_1 = \begin{pmatrix} 0 & 1 \\ 0 & 0 \end{pmatrix}; A_2 = 0 ; B_1 = \begin{pmatrix} 0 \\ 1 \end{pmatrix}; B_2 = 1$$

Inserting (9) and (10) into (8), we get the control voltages u_q and u_d :

$$\begin{pmatrix} u_q \\ u_d \end{pmatrix} = \Delta^{-1}(x) \times \left[-\Delta_0(x) + \begin{pmatrix} -k_{11}(y_1 - y_{1d}) - k_{12}(\dot{y}_1 - \dot{y}_{1d}) + \ddot{y}_{1d} \\ -k_2(y_2 - y_{2d}) + \dot{y}_{2d} \end{pmatrix} \right]$$

4 Block diagram on MATLAB/Simulink and simulation results

In this section, we present the simulation results of the proposed control. Before this, Figure 2 shows the structure of the PMSM control by linearization and input-output decoupling via static state feedback. We have used the PMSM model integrated in MATLAB/Simulink associated with a PWM-controlled voltage inverter.

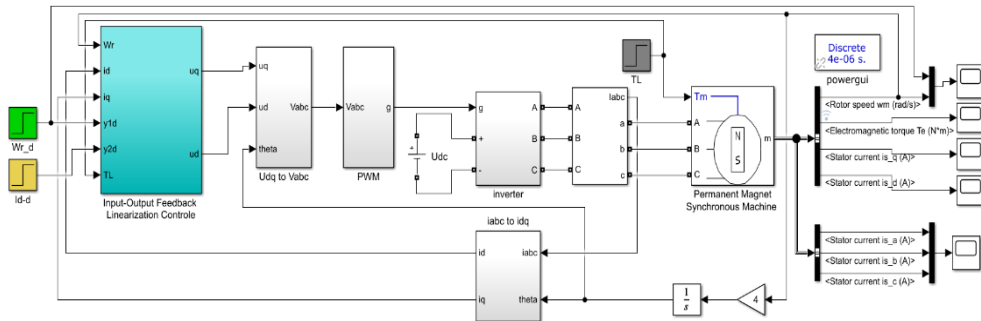


Fig 2. Global control scheme for the PMSM by Input-Output Feedback Linearization

The parameters and nominal values of the PMSM used are identical to those described in the paper [3]. They are shown in Table 1.

Table 1. The PMSM parameters.

| Parameters | Values |
|------------------------------------|--------|
| DC Link voltage [V] | 220 |
| Rated power [KW] | 1.1 |
| Rated speed [rpm] | 3000 |
| Permanent magnet flux [Wb] | 0.175 |
| Pole pairs number | 4 |
| Viscous friction coefficient [Nms] | 0.0008 |
| Motor inertia [Kgm ²] | 0.001 |
| Stator phase resistance [Ω] | 2.875 |
| Stator phase inductances [mH] | 8.5 |

Figures 3(a)-(h) show the simulated responses obtained by closed-loop regulation of the chosen control. This is done in order to examine and give concrete reality to the performance of this control technique. These simulations include scenarios where a sudden change in speed and a sudden increase in load torque are applied to the permanent magnet synchronous motor. The motor starts with a load torque of 3 Nm and an initial speed step of 94.247 rad/s (900 rpm), with the reference speed abruptly increased to 125.66 rad/s (1200 rpm) at 0.05

seconds. At 0.1 seconds, an instantaneous application of a 7 Nm load torque to the motor is observed in Figure 3(g).

Figures 3(a)-(d) show that the rotor speed of the PMSM converges to the desired value with a response time of approximately 6 milliseconds and without transient overshoot. However, it is worth noting that the static error in steady-state remains relatively low, not exceeding 0.23 rad/s. Figure 3(h) shows the currents of phases A, B and C, displaying rapid variations in amplitude as a result of changes in load torque or speed.

Figure 3(f) shows that during start-up, a significant overshoot of the q-axis current occurs, with the current peaking at 23 A before stabilizing at its nominal value. On the other hand, the d-axis current rapidly converges to zero and remains close to 0A, so that the electromagnetic torque produced by the motor is proportional to the q-axis current (see equation (5)). Obviously, decoupling is guaranteed. The impact of the sudden load torque disturbance on rotor speed is evident in figure 3(d), as the speed suffers a transient drop of between 2 and 3 rad/s when the load is applied (see figure 3(g)).

These figures collectively demonstrate the ability of the linearization and input-output feedback control technique to compensate the load torque disturbance.

The actual motor parameters are not perfectly known due to practical conditions and identification errors, for example: variation in stator resistance caused by temperature changes; uncertainty in inductance is very common due to the non-linear characteristics of the magnetic circuit; operation at low rotational speeds; variation in inertia caused by increasing load [3]. Several studies have shown that parameter uncertainties degrade control performance and can reduce drive robustness [8,15]. A $\pm 50\%$ variation in the nominal value of resistance, stator inductance and moment of inertia, as well as a 20% variation in magnet flux, was carried out under conditions of load torque disturbance increasing from the value 3 Nm to 7 Nm at 50 milliseconds, thereby proving the robustness of the IOFL control. For each scenario, reference speed is ramps to a steady 110 rad/s (1050 rpm), and speed error is shown in Figures 4(a)-(b) to 7(a)-(b). From the graphs, we can see that the steady-state static error remains limited to ± 1 rad/s. These results highlight one of the limitations of linearized feedback control against parametric PMSM perturbations.

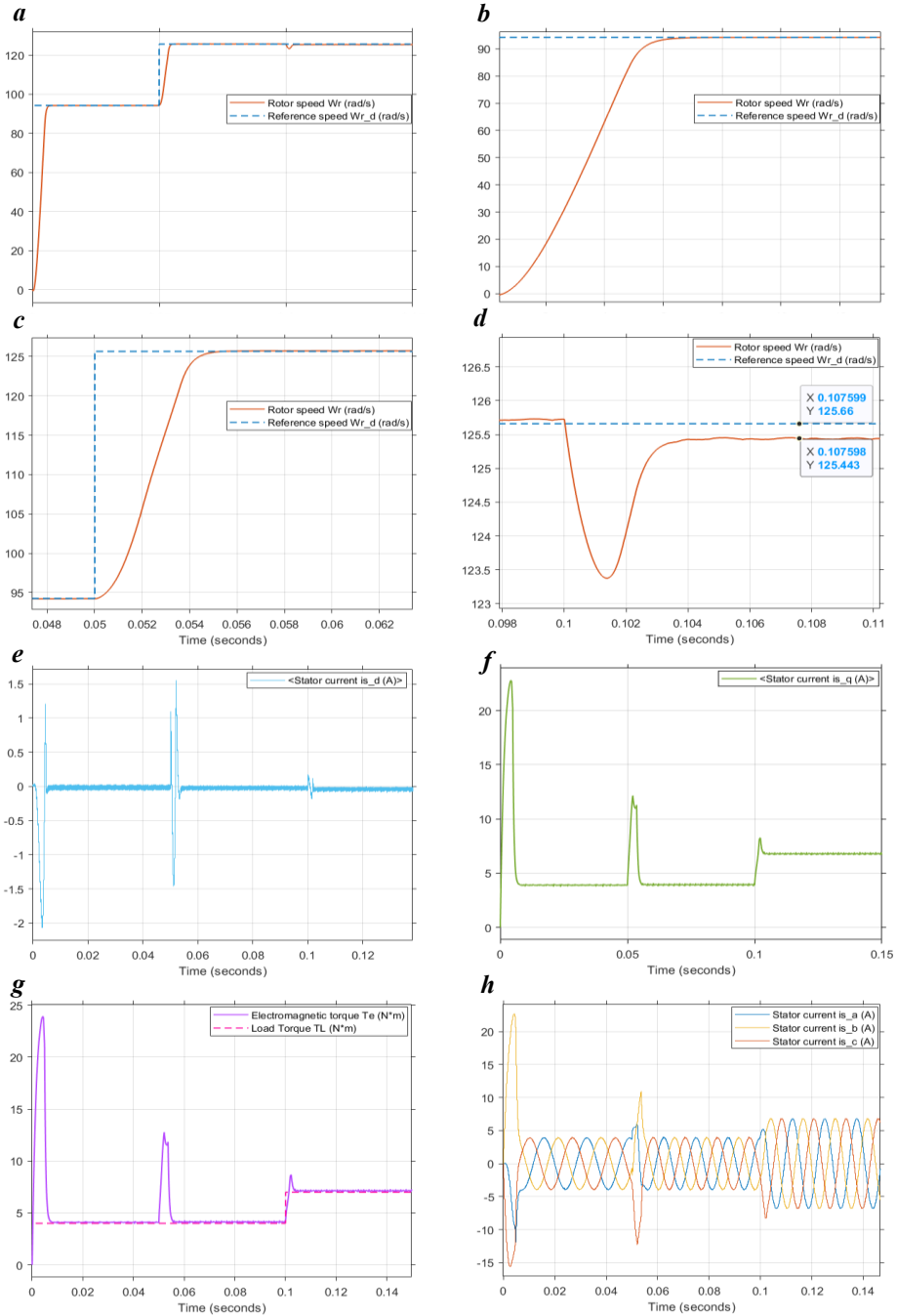


Fig 3. Simulated training data was used to examine the response of sudden acceleration at 0.05s and increasing load torque at 0.1s. Elements analyzed included: (a) Velocity tracking response for a step reference profile; (b) Zoom to the region near 0s; (c) Zoom around 0.05s; (d) Zoom around 0.1s; (e) Direct current; (f) Quadrature current; (g) Electromagnetic torque and load torque; and (h) Stator currents of the three phases A, B and C.

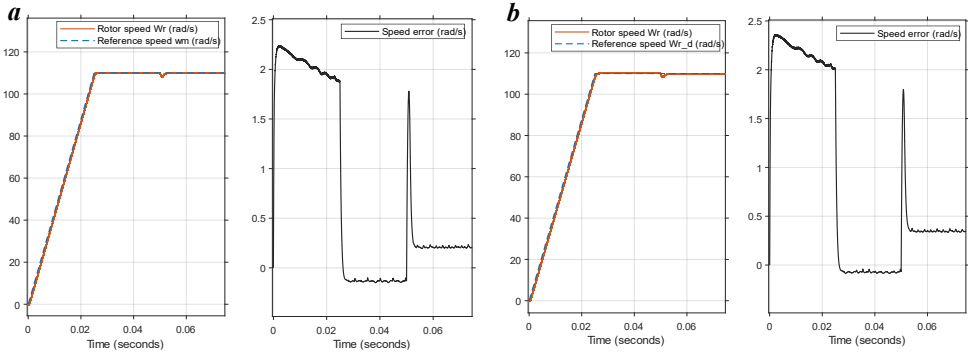


Fig 4. Changes in stator resistance R_s . (a) +50 % R_s ; (b) -50 % R_s

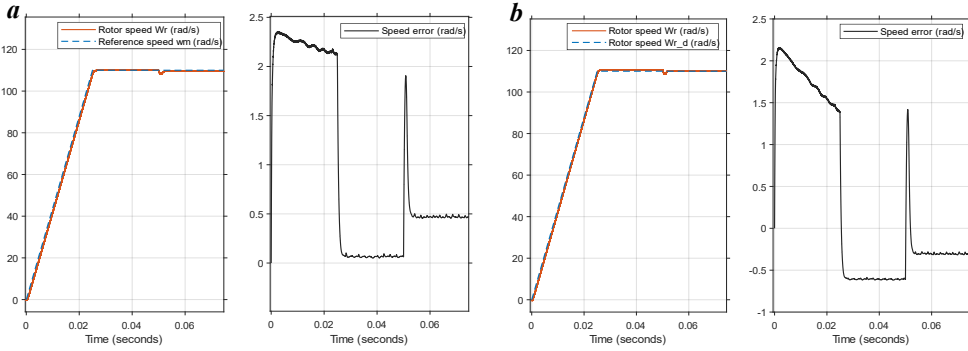


Fig 5. Changes in stator inductance L_s . (a) +50 % L_s ; (b) -50 % L_s

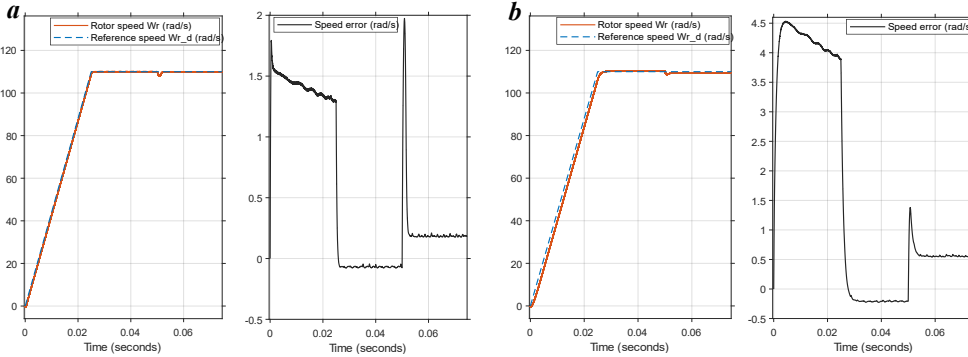


Fig 6. Changes in rotor inertia J . (a) +50 % J ; (b) -50 % J

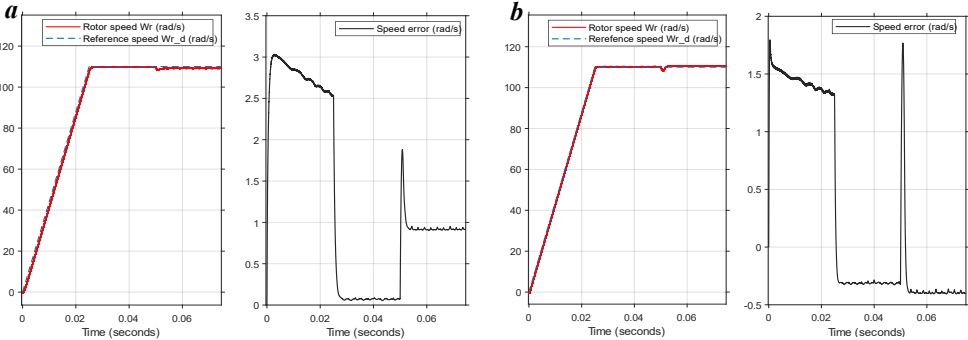


Fig 7. Changes in rotor flux ϕ_r . (a) +20 % ϕ_r ; (b) -20 % ϕ_r

5 Conclusion and prospects

The linearization and input-output decoupling method requires a well-defined model and, in many cases, allows compensation for a certain non-linearity, which can be useful. However, the validity of the proposed control is confirmed by the simulation results obtained, with rotor speed and direct current converging to their desired values with acceptable static and dynamic behaviour. However, it suffers against PMSM parameter variations, as well as some limitations at low rotational speeds due to significant non-linearities such as magnetic saturation of permanent magnets and iron losses, which make accurate modelization difficult and consequently affect the performance of exact linearization control. To address this, it is obvious to consider an adaptive control technique based on real-time observation of PMSM parameters or advanced algorithms based on artificial intelligence such as neural network methods should clearly be considered.

Abbreviations

| | |
|----------------|--|
| <i>SM PMSM</i> | <i>Surface Mounted Permanent Magnet Synchronous Motors</i> |
| <i>SMC</i> | <i>Sliding Mode Control</i> |
| <i>DTC</i> | <i>Direct Torque Control</i> |
| <i>ADRC</i> | <i>Active Disturbance Rejection Control</i> |
| <i>PWM</i> | <i>Pulse Width Modulation</i> |

References

- [1] K. Zhou, M. Ai, D. Sun, N. Jin, et X. Wu, « Field Weakening Operation Control Strategies of PMSM Based on Feedback Linearization », *Energies*, vol. 12, n° 23, p. 4526, nov. 2019, doi: 10.3390/en12234526.
- [2] M. A. Hamida, J. de Leon, et A. Glumineau, « Experimental sensorless control for IPMSM by using integral backstepping strategy and adaptive high gain observer », *Control Eng. Pract.*, vol. 59, p. 64-76, févr. 2017, doi: 10.1016/j.conengprac.2016.11.012.
- [3] A. Senhaji, M. Abdelouhab, A. Attar, et J. Bouchnaif, « Backstepping control of a permanent magnet synchronous motor », *Mater. Today Proc.*, vol. 72, p. 3730-3737, 2023, doi: 10.1016/j.matpr.2022.09.248.
- [4] S. Rebouh, A. Kaddouri, R. Abdessemed, et A. Haddoun, « Nonlinear Control by Input-Output Linearization Scheme for EV Permanent Magnet Synchronous Motor », in *2007 IEEE Vehicle Power and Propulsion Conference*, Arlington, TX, USA: IEEE, sept. 2007, p. 185-190. doi: 10.1109/VPPC.2007.4544122.
- [5] W. Gu, X. Zhu, L. Quan, et Y. Du, « Design and Optimization of Permanent Magnet Brushless Machines for Electric Vehicle Applications », *Energies*, vol. 8, n° 12, p. 13996-14008, déc. 2015, doi: 10.3390/en81212410.
- [6] P. Jayal, S. Rawat, et G. Bhuvanawari, « Simplified Sensor Based Vector Control of Permanent Magnet Synchronous Motor Drive », in *2020 IEEE International Conference on Power Electronics, Smart Grid and Renewable Energy (PESGRE2020)*, Cochin, India: IEEE, janv. 2020, p. 1-6. doi: 10.1109/PESGRE45664.2020.9070639.
- [7] Kaddouri, Akhrif, Hoang Le-Huy, et Ghribi, « Nonlinear feedback control of a permanent magnet synchronous motors », in *Proceedings of Canadian Conference on Electrical and Computer Engineering CCECE-94*, Halifax, NS, Canada: IEEE, 1994, p. 77-80 vol.1. doi: 10.1109/CCECE.1994.405657.
- [8] M. Karabacak et H. I. Eskikurt, « Speed and current regulation of a permanent magnet synchronous motor via nonlinear and adaptive backstepping control », *Math. Comput. Model.*, vol. 53, n° 9-10, p. 2015-2030, mai 2011, doi: 10.1016/j.mcm.2011.01.039.
- [9] Z. Wu, Y. Shen, T. Pan, et Z. Ji, « Feedback linearization control of PMSM based on differential geometry theory », in *2010 5th IEEE Conference on Industrial Electronics and Applications*, Taichung, Taiwan: IEEE, juin 2010, p. 2047-2051. doi: 10.1109/ICIEA.2010.5515457.

- [10] Z. Meng, C. Sun, Y. An, et J. Cao, « Non-Interacting Control of PMSM Based on Exact Linearization Via State Variable Feedback », in *2009 International Workshop on Intelligent Systems and Applications*, Wuhan, China: IEEE, mai 2009, p. 1-4. doi: 10.1109/IWISA.2009.5072974.
- [11] S. Xiao-jing, « Design and Simulation of PMSM Feedback Linearization Control System », *TELKOMNIKA Indones. J. Electr. Eng.*, vol. 11, n° 3, p. 1245-1250, mars 2013, doi: 10.11591/telkommika.v11i3.2192.
- [12] C. Liu et J. Zhai, « Global adaptive event-triggered output feedback controller design for high-order nonlinear systems », *J. Frankl. Inst.*, vol. 360, n° 3, p. 1540-1559, févr. 2023, doi: 10.1016/j.jfranklin.2022.12.026.
- [13] M. Morawiec, « The Adaptive Backstepping Control of Permanent Magnet Synchronous Motor Supplied by Current Source Inverter », *IEEE Trans. Ind. Inform.*, vol. 9, n° 2, p. 1047-1055, mai 2013, doi: 10.1109/TII.2012.2223478.
- [14] M. Karabacak et H. I. Eskikurt, « Design, modelling and simulation of a new nonlinear and full adaptive backstepping speed tracking controller for uncertain PMSM », *Appl. Math. Model.*, vol. 36, n° 11, p. 5199-5213, nov. 2012, doi: 10.1016/j.apm.2011.12.048.
- [15] J. Zhou et Y. Wang, « Adaptive backstepping speed controller design for a permanent magnet synchronous motor », *IEE Proc. - Electr. Power Appl.*, vol. 149, n° 2, p. 165, 2002, doi: 10.1049/ip-epa:20020187.
- [16] X. Sun, H. Yu, J. Yu, et X. Liu, « Design and implementation of a novel adaptive backstepping control scheme for a PMSM with unknown load torque », *IET Electr. Power Appl.*, vol. 13, n° 4, p. 445-455, avr. 2019, doi: 10.1049/iet-epa.2018.5656.
- [17] M. Ezzat, A. Glumineau, et F. Plestan, « Sensorless high order sliding mode control of permanent magnet synchronous motor », in *2010 11th International Workshop on Variable Structure Systems (VSS)*, Mexico City, Mexico: IEEE, juin 2010, p. 233-238. doi: 10.1109/VSS.2010.5544687.
- [18] A. Hezzi, Y. Bensalem, S. Ben Elghali, et M. Naceur Abdelkrim, « Sliding Mode Observer based sensorless control of five phase PMSM in electric vehicle », in *2019 19th International Conference on Sciences and Techniques of Automatic Control and Computer Engineering (STA)*, Sousse, Tunisia: IEEE, mars 2019, p. 530-535. doi: 10.1109/STA.2019.8717290.
- [19] A. Ammar, A. Bourek, et A. Benakcha, « Nonlinear SVM-DTC for induction motor drive using input-output feedback linearization and high order sliding mode control », *ISA Trans.*, vol. 67, p. 428-442, mars 2017, doi: 10.1016/j.isatra.2017.01.010.
- [20] B. Ning, S. Cheng, et Y. Qin, « Direct torque control of PMSM using sliding mode backstepping control with extended state observer », *J. Vib. Control*, vol. 24, n° 4, p. 694-707, févr. 2018, doi: 10.1177/10775463166650097.
- [21] F. Deng et Y. Guan, « PMSM Vector Control Based on Improved ADRC », in *2018 IEEE International Conference of Intelligent Robotic and Control Engineering (IRCE)*, Lanzhou: IEEE, août 2018, p. 154-158. doi: 10.1109/IRCE.2018.8492927.
- [22] G. Su, « Fuzzy ADRC Controller Design for PMSM Speed Regulation System », *Adv. Mater. Res.*, vol. 201-203, p. 2405-2408, févr. 2011, doi: 10.4028/www.scientific.net/AMR.201-203.2405.
- [23] S. Zhou, Y. Li, et S. Tong, « Finite-time adaptive neural network event-triggered output feedback control for PMSMs », *Neurocomputing*, vol. 533, p. 10-21, mai 2023, doi: 10.1016/j.neucom.2023.02.039.
- [24] Y. Dai, S. Ni, D. Xu, L. Zhang, et X.-G. Yan, « Disturbance-observer based prescribed-performance fuzzy sliding mode control for PMSM in electric vehicles », *Eng. Appl. Artif. Intell.*, vol. 104, p. 104361, sept. 2021, doi: 10.1016/j.engappai.2021.104361.
- [25] L. Wang, H. Zhang, et X. Liu, « SLIDING MODE VARIABLE STRUCTURE I/O FEEDBACK LINEARIZATION DESIGN FOR THE SPEED CONTROL OF PMSM WITH LOAD TORQUE OBSERVER », p. 12.
- [26] J. Zhang, Z. Meng, R. Chen, C. Sun, et Y. An, « Decoupling control of PMSM based on exact linearization », in *Proceedings of 2011 International Conference on Electronic & Mechanical Engineering and Information Technology*, Harbin, Heilongjiang, China: IEEE, août 2011, p. 1458-1461. doi: 10.1109/EMEIT.2011.6023323.